

Rise and Fall of Multifragment Emission

C. A. Ogilvie,⁽¹⁾ J. C. Adloff,⁽⁶⁾ M. Begemann-Blaich,⁽¹⁾ P. Bouissou,⁽⁵⁾ J. Hubele,⁽¹⁾ G. Imme,⁽⁴⁾ I. Iori,⁽⁷⁾ P. Kreuz,⁽²⁾ G. J. Kunde,⁽¹⁾ S. Leray,⁽⁵⁾ V. Lindenstruth,⁽¹⁾ Z. Liu,⁽¹⁾ U. Lynen,⁽¹⁾ R. J. Meijer,⁽¹⁾ U. Milkau,⁽¹⁾ W. F. J. Müller,⁽¹⁾ C. Ngô,⁽⁵⁾ J. Pochodzalla,⁽²⁾ G. Raciti,⁽⁴⁾ G. Rudolf,⁽⁶⁾ H. Sann,⁽¹⁾ A. Schüttauf,⁽²⁾ W. Seidel,⁽³⁾ L. Stuttge,⁽⁶⁾ W. Trautmann,⁽¹⁾ and A. Tucholski⁽²⁾

⁽¹⁾*Gesellschaft für Schwerionenforschung, D-6100 Darmstadt, Federal Republic of Germany*

⁽²⁾*Institut für Kernphysik, Universität Frankfurt, D-6000 Frankfurt, Federal Republic of Germany*

⁽³⁾*Zentralinstitut für Kernforschung, Rossendorf, Dresden, Federal Republic of Germany*

⁽⁴⁾*Dipartimento di Fisica dell'Università, I-95129 Catania, Italy*

⁽⁵⁾*Laboratoire National Saturne, Centre d'Etudes Nucléaires de Saclay, F-91191 Gif-sur-Yvette, France*

⁽⁶⁾*Centre de Recherches Nucléaires, Strasbourg, France*

⁽⁷⁾*Istituto di Scienze Fisiche, Università degli Studi di Milano, I-20133 Milano, Italy*

(Received 27 March 1991)

We have studied multifragment decays of Au projectiles after collisions with C, Al, and Cu targets at a bombarding energy of 600 MeV/nucleon. We find that with increasing violence of the collision, measured via the multiplicity of light particles, the mean multiplicity of intermediate-mass fragments originating from the projectile first increases to a maximum $\langle M_{\text{IMF}} \rangle \approx 3$ and then decreases again. Calculations using the Boltzmann-Uehling-Uhlenbeck model suggest that the fragmentation is governed by the energy E_{dep} deposited into the projectile spectator and that $\langle M_{\text{IMF}} \rangle$ reaches its maximum around $E_{\text{dep}} \approx 8$ MeV/nucleon.

PACS numbers: 25.70.Np

When a nucleus is excited to and beyond its total binding energy, it is predicted to decay into several intermediate-mass fragments (IMFs). Competing models embody different decay mechanisms and experiments have yet to discriminate between several theoretical scenarios. These range from the near simultaneous emission of fragments due to large fluctuations in regions of mechanical instability [1,2], to statistical multifragmentation models [3,4], and sequential decay processes where equilibrium is reestablished after each binary decay [5,6].

In order to constrain and confront these models, it is important to know under what conditions fragments are emitted. Is there an excitation energy at which multifragment emission begins to be a dominant process, and what happens if the excitation is increased further? Eventually the energy will be so large that the system will disassemble into nucleons and light fragments such as α particles. Hence one expects a rise and fall of multifragment emission with excitation energy.

One of the early results on multifragmentation came from the inclusive charge distribution of fragments emitted from proton-induced reactions [7]. The observation of a minimum of the τ parameter ($\sigma \sim Z^{-\tau}$) was interpreted as evidence for a liquid-gas phase transition. This interpretation is disputed [8,9] partly because the measurement is an average over all impact parameters. It is important to extend these studies by selecting the impact parameter of the collision and measuring the multiplicity of the fragments as well as their charge distribution.

We use asymmetric nuclear collisions at relativistic energies to excite a large nucleus [10]. A schematic reaction mechanism is that the initial nucleon-nucleon collisions form a fireball and that some of these nucleons traverse through the larger nucleus. As these undergo

secondary collisions they excite the large nucleus. In the second stage of the reaction, this excited "spectator" nucleus decays into a variety of exit channels, some of which will be multifragment states. Previous experimental results are consistent with this reaction mechanism, and show that fragments are emitted nearly isotropically from an excited source that moves with a velocity near that of the initial velocity of the larger nucleus [11,12].

We report on semiexclusive data of fragments emitted in Au reactions on three light targets, C, Al, and Cu at a beam energy of 600 MeV/nucleon. The experiment was performed with the ALADIN forward spectrometer [13] at GSI, Darmstadt, with the beam accelerated by the SIS synchrotron. The inverse kinematics have the effect that the fragments from the Au projectile are focused into the forward direction. The beam rate was approximately 2000 particles during a 500-ms spill and the targets were 200 to 500 mg/cm² thick. A 64-element Si-CsI array measured the multiplicity of light charged particles (M_{CSi}) with a solid angle coverage of approximately 50% between $\theta = 7^\circ$ and 25° and 15% between $\theta = 25^\circ$ and 40° .

The ALADIN magnet was operated at a bending power of 1.4 Tm and the acceptance for beam-velocity $N=Z$ fragments was $\pm 4.7^\circ$ in the horizontal and $\pm 4.2^\circ$ in the vertical direction. The TP-MUSIC detector [13] was used in this analysis to calibrate the charge measured in the TOF wall. The TOF wall consisted of two layers, each of forty vertical scintillator strips that are 1.1 m long and 2.5 cm wide. The distance from the target was approximately 6 m. The two TOF layers were displaced from each other in the bending plane by one-half of a strip's width. This leaves no inactive area between the strips. The TOF wall is used in this work to

TABLE I. Summary of experimental results for Au 600-MeV/nucleon collisions on C, Al, and Cu targets. For each target, the average maximum charge in each event, the τ parameter from the charge distributions, and the mean multiplicity of intermediate-mass fragments are given for peripheral (top row), mid-central, and central (bottom row) collisions. The uncertainties for $\langle M_{\text{IMF}} \rangle$ correspond to the statistical and systematic errors, respectively. The first column gives the multiplicity cuts used in the CsI array, and the second column is the estimated mean and the half width at half maximum of the impact-parameter selection for each class of reaction.

	M_{CsI}	$\langle b \rangle$ (fm)	$\langle Z_{\text{max}} \rangle$	τ	$\langle M_{\text{IMF}} \rangle$
C	1-5	7.5 ± 1.5	56 ± 2	2.8 ± 0.2	$0.93 \pm 0.03 \pm 0.09$
	6-10	5.5 ± 2	38 ± 1	2.2 ± 0.1	$2.31 \pm 0.06 \pm 0.21$
	≥ 11	3.5 ± 2	25 ± 1	2.0 ± 0.1	$3.39 \pm 0.11 \pm 0.37$
Al	1-8	8 ± 1.5	53 ± 2	2.6 ± 0.1	$1.13 \pm 0.03 \pm 0.10$
	9-16	5 ± 2	26 ± 1	2.0 ± 0.1	$3.00 \pm 0.05 \pm 0.26$
	≥ 17	3 ± 1.5	12 ± 0.5	2.1 ± 0.1	$3.30 \pm 0.08 \pm 0.17$
Cu	1-9	9 ± 1.5	53 ± 2	2.6 ± 0.1	$1.14 \pm 0.04 \pm 0.10$
	10-21	6 ± 2	20 ± 1	2.0 ± 0.1	$2.96 \pm 0.07 \pm 0.20$
	≥ 22	3 ± 1.5	6 ± 0.5	2.6 ± 0.1	$1.97 \pm 0.07 \pm 0.09$

determine the charge and multiplicity of nuclear fragments with $Z \geq 2$. Unit charge resolution was obtained for $Z < 9$, increasing to a charge resolution of ± 1.5 at $Z = 79$.

The TOF strips near 0° provided an interaction trigger, and off-line the events have been placed into three groups according to M_{CsI} . This multiplicity is expected to be a measure of the size of the fireball formed in the initial stage of the reaction and hence a measure of the impact parameter. The borders of the three groups have been set (see Table I) such that the peripheral (lowest multiplicity), mid-central, and central groups have 50%, 35%, and 15% of the events, respectively. The average M_{CsI} is estimated to be 40% of the true charged-particle multiplicity in this angular range. This inefficiency is approximately independent of the target and impact parameter because the measured angular distribution within the array is qualitatively similar for all impact groups. The multiplicity cuts retain an average correspondence with the impact parameter because they have been chosen such that the widths of these cuts are at least as large as the estimated fluctuations. For the highest-multiplicity group on each target, this has been achieved by setting the cut well before the tail of the distribution. Additional support for the usefulness of M_{CsI} as an impact-parameter filter comes from the correlation of M_{CsI} with other observables that are related to the impact parameter, e.g., the largest fragment in the event. These correlations, as well as theoretical predictions of the measured multiplicity, are discussed in Ref. [14].

In Fig. 1 we present the charge distributions for the targets C, Al, and Cu. These distributions have been corrected for the loss of efficiency due to our finite coverage, with the correction being of the order 5% for $Z = 3$ fragments and less than 2% for $Z > 6$. The inefficiency has been evaluated separately for each target and

impact-parameter group [14]. The absolute normalization was determined by counting beam particles at the target; this normalization has an accuracy of 15%. For all targets, there is a strong reduction of yield of fragments with $Z > 30$ with increasing M_{CsI} , i.e., as one goes from peripheral to central reactions. For fragments with $Z < 30$, the distribution is steep in peripheral reactions, which is characteristic of light-fragment evaporation from a heavy system. On the C target, the $Z < 30$ distribution is considerably broader for both mid-central and central collisions, i.e., the relative probability for emitting heavier fragments is greater. For reactions on Al, the mid-central distribution is similar to the distribution for

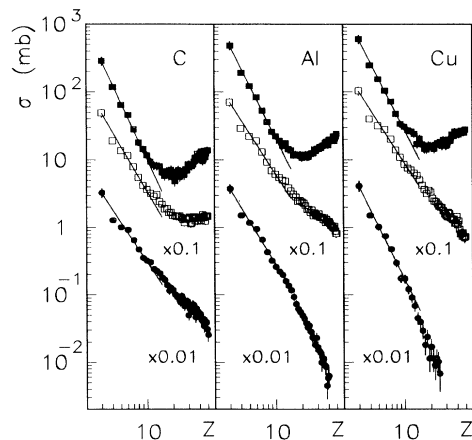


FIG. 1. The measured charge distributions from $Z = 3$ for Au 600-MeV/nucleon collisions on C, Al, and Cu targets. The solid square data points are for peripheral collisions, the open squares for mid-central collisions, and the solid circles for central collisions. The lines are from the power-law fit and are plotted for $3 \leq Z \leq 15$.

central reactions on the C target. On the Cu target, the mid-central collisions produce a broad distribution, while the central reactions produce predominantly lighter fragments. These distributions were fitted with a power law ($\sigma \sim Z^{-\tau}$) for $Z=3$, $5 \leq Z \leq 15$, and the extracted τ parameters are listed in Table I.

We define an IMF as a fragment with $3 \leq Z \leq 30$. In Fig. 2 we plot the correlation between the multiplicity of IMFs and M_{Csl} . For the C target, the IMF multiplicity increases with the violence of the collision and reaches a mean multiplicity of 3 to 4 for the most central collisions. The reactions on Al behave similarly in that three to four IMFs are emitted; however, this occurs over a broader range of M_{Csl} . For the Cu target, the region of three to four IMFs is reached for lower relative M_{Csl} . With more violent collisions, the multiplicity of IMFs reduces to 1 or 2. For each impact-parameter group, we have evaluated the mean IMF multiplicity and applied a (3-5)% correction for the finite coverage. This correction has been evaluated separately for each impact-parameter group. The double-hit probability is of the order of 10% which leads to some misidentification of fragments. This has been included in the systematic error of the IMF multiplicity. We have summarized our results in Table I, where we have also included the estimated range of impact parameters for each group [14].

For the most central collisions on Cu, a decrease in the multiplicity of IMFs can result from charge conservation. The formation of the fireball removes charge from the projectile, an effect which increases with centrality. The size of the projectile spectator can be estimated from M_{Csl} , the geometrical coverage of the CsI array, and the relative contribution of target and projectile nucleons to the fireball. For mid-impact collisions on copper ($\langle Z_{\text{spec}} \rangle \sim 58 \pm 5$), and for central collisions ($\langle Z_{\text{spec}} \rangle \sim 40 \pm 7$). Statistical-model calculations [4] predict that the de-

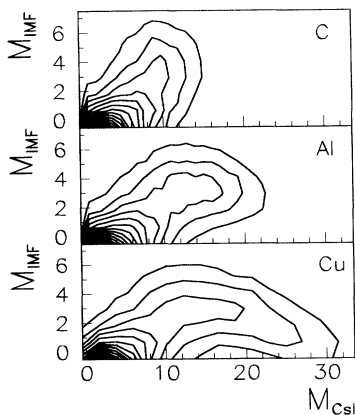


FIG. 2. The measured correlation of the multiplicity of IMFs at forward angles with M_{Csl} . The results are for 600 MeV/nucleon Au on C, Al, and Cu and the contours are drawn using a linear scale.

crease in IMF multiplicity is 0.025 times the decrease of the initial charge of a decaying nucleus for a fixed excitation energy per nucleon. Hence the expected IMF multiplicity decrease, due to charge conservation, of $\Delta \langle M_{\text{IMF}} \rangle = -0.5 \pm 0.3$ can only partially explain the observed fall of $\langle M_{\text{IMF}} \rangle$ (Fig. 2 and Table I). Given our current errors, it is, however, important to confirm this result with experiments that can measure the size of the spectator more accurately.

The results in Table I can be directly compared to dynamical models that produce fragments, such as quantum molecular dynamics [9]. To facilitate comparisons with fragmentation models that do not include the reaction dynamics, and to help interpret these experimental observations, we have performed a series of calculations with a Boltzmann-Uehling-Uhlenbeck (BUU) model [15]. We have used the model to calculate the energy deposited into the projectile during the initial stage of the reaction. Similar approaches have been used in Refs. [16] and [17].

A projectile spectator is defined as all the nucleons within a sphere in coordinate space, where the position and size of the sphere is calculated from the distribution of projectile nucleons that have yet to undergo a nucleon-nucleon collision. The deposited energy is calculated from the momentum and potential energy of the nucleons within this sphere minus an estimate of the ground-state energy. The deposited energy per nucleon varies by less than 10% between 60 and 100 fm/c after the onset of the reaction. By 60 fm/c most of the fireball-like nucleons have left the reaction zone. An

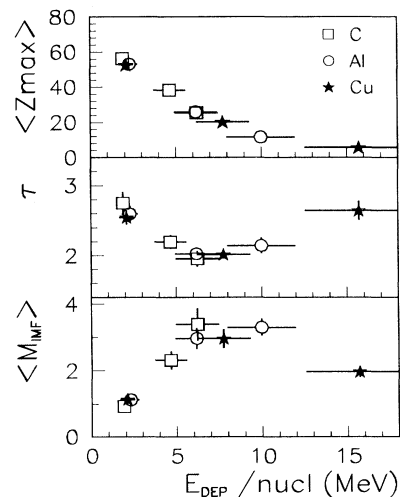


FIG. 3. The average maximum charge in each event, the fitted τ parameter from the charge distribution, and the mean IMF multiplicity plotted vs the calculated deposited energy per nucleon. The squares, circles, and stars represent collisions on the C, Al, and Cu targets, respectively. Each point within a target group corresponds to peripheral, mid-central, and central collisions with the deposited energy increasing with centrality.

average deposited energy was calculated during this time interval (60–100 fm/c) for all targets and impact parameters. For central, mid-central, and peripheral reactions a further average is taken over the impact-parameter ranges in Table I. The number of nucleons within the sphere decreases from approximately 180 for peripheral collisions to 100 for central collisions on Cu. The error for the deposited energy has been estimated by changing the radius of the spectator sphere by 10%, using different intervals when averaging over both time and impact parameter, and by noting that the energy nonconservation of the model during 100 fm/c is less than 0.2 MeV/nucleon.

In Fig. 3 we plot the maximum charge in an event, the fitted τ parameter from the charge distribution, and the mean IMF multiplicity versus the calculated deposited energy per nucleon. For systems at low energy there is a heavy residue, a steep charge distribution, i.e., large τ parameter, and small IMF multiplicity. As the energy increases, the number of emitted IMFs increases, the charge distribution broadens, and the maximum charge in an event decreases. At still higher energies, the maximum charge in the event becomes quite small and the multiplicity of IMFs decreases. In their place lighter fragments are produced as deduced from an increase in τ . Again, part of these changes at high deposited energy can be attributed to the decreasing size of the projectile spectator.

The universal behavior of the experimental results over the full range of the calculated deposited energy suggests that this energy might be a significant parameter that drives the decay of the projectile nucleus. The deposited energy is model dependent, but this dependence is expected to affect the scale of the deposited energy, and should not change the ordering of targets and impact parameters. For reactions leading to excitations of up to ~ 3 MeV/nucleon, the role of the deposited energy in governing fragment emission has been experimentally established [18].

In summary, we have experimentally determined a set of optimum conditions for the multifragment decay of a large nucleus. For asymmetric reactions at 600 MeV/nucleon, multifragment emission is the dominant decay

channel for the most violent collisions on a light target and for mid-central collisions on a heavy target. In peripheral collisions, a heavy residue and lighter fragments are observed. In central collisions on heavy targets, only light fragments are produced. It is now a challenge to confront the various models of multifragmentation with these systematics.

The authors thank W. Bauer for the use of the BUU code and useful discussions. We acknowledge discussions with R. J. Lenk.

Note added.—After submitting this Letter, we became aware of recent work that examines the rise of multifragment emission in Xe+Au collisions at 50 MeV/nucleon [19].

-
- [1] G. Bertsch and P. J. Siemens, Phys. Lett. **126B**, 9 (1983).
 - [2] C. J. Pethick and D. G. Ravenhall, Nucl. Phys. **A471**, 19c (1987).
 - [3] D. H. E. Gross and H. Massman, Nucl. Phys. **A471**, 339c (1987).
 - [4] H. W. Barz *et al.*, Phys. Lett. **169B**, 318 (1986).
 - [5] W. A. Friedman and W. G. Lynch, Phys. Rev. C **28**, 16 (1983).
 - [6] R. J. Charity *et al.*, Nucl. Phys. **A483**, 371 (1988).
 - [7] N. T. Porile *et al.*, Phys. Rev. C **39**, 1914 (1989), and references therein.
 - [8] J. Aichelin and J. Huefner, Phys. Lett. **136B**, 15 (1984).
 - [9] G. Peilert *et al.*, Phys. Rev. C **39**, 1402 (1989).
 - [10] R. Stock *et al.*, Phys. Rev. Lett. **44**, 1243 (1980).
 - [11] A. I. Warwick *et al.*, Phys. Rev. C **27**, 1083 (1983).
 - [12] S. J. Yennello *et al.*, Phys. Lett. **B 246**, 26 (1990).
 - [13] ALADIN Collaboration, U. Lynen *et al.*, Gesellschaft für Schwerionenforschung Report No. GSI-02-89 (unpublished).
 - [14] J. Hubele *et al.*, Z. Phys. A (to be published).
 - [15] G. F. Bertsch and S. das Gupta, Phys. Rep. **160**, 189 (1988).
 - [16] E. Suraud *et al.*, Nucl. Phys. **A495**, 73c (1989).
 - [17] A. S. Botvina, A. S. Iljinov, and I. N. Mishustin, Nucl. Phys. **A507**, 649 (1990).
 - [18] R. Trockel *et al.*, Phys. Rev. C **39**, 729 (1989).
 - [19] D. Bowman *et al.*, Michigan State University Report No. MSUCL-779, 1991 (to be published).